Electronic Supplementary Material (ESI) for Physical Chemistry Chemical Physics.
This journal is © the Owner Societies 2023

Electronic Supplementary Information: Does HNO_3 dissociate on gas-phase ice nanoparticles?

Anastasiya Khramchenkova,[a] Andriy Pysanenko,[b] Jozef Ďurana,[b] Barbora Kocábková,[b] Michal Fárník,*[b] and Jozef Lengyel*[a]

[a]Lehrstuhl für Physikalische Chemie, TUM School of Natural Sciences, Technische Universität München, Lichtenbergstraße 4, 85748 Garching, Germany. E-mail: jozef.lengyel@tum.de

[b]J. Heyrovský Institute of Physical Chemistry v.v.i., Czech Academy of Sciences, Dolejškova 3, 18223 Prague, Czech Republic. E-mail: michal.farnik@jh-inst.cas.cz

1. Experimental details

The cluster experiments were carried out on the CLUster Beam (CLUB) apparatus in the J. Heyrovsky Institute of Physical Chemistry in Prague described in our previous reviews[1–3] and references cited therein. The details particular to the present experiments are outlined below.

In the pickup experiments, the water clusters were produced by a supersonic expansion of water vapor through a divergent conical nozzle of 90 μm diameter with a length of 2 mm and 30° full opening angle into a high vacuum. The water reservoir with the attached nozzle was placed in the source vacuum chamber and heated to independent controlled temperatures T_R and T_N, respectively. The reservoir temperature T_R determined the water vapor pressure and the nozzle temperature T_N was kept somewhat higher to prevent the water condensation in the nozzle. The mean size $\bar{N}$ of the water clusters $(H_2O)_N$ was well established in previous experiments with the same water cluster source,[4] and could be calculated from the expansion conditions according to a modified Hagena's formula[4,5]. In the present experiments, the mean cluster sizes were from $\bar{N} \approx 30$ to 470, and for the spectrum shown in the main article in Fig. 1, it was $\bar{N} \approx 180$. After passing through a skimmer of 1 mm in diameter, the water cluster beam entered a differentially pumped pickup chamber filled with HNO_3/H_2O vapor at a pressure of about $1{\times}10^{-4}$ mbar. The pickup conditions are analyzed below and correspond to the probability of less than one for the pickup of an HNO_3 molecule by an average $(H_2O)_{\bar{N}}$, $\bar{N} \approx 180$, cluster.

The expansion conditions to produce the mixed HNO_3/H_2O clusters in the comparative experiments were essentially the same as in our previous studies of the mixed $(HNO_3)_M(H_2O)_N$ clusters.[6–8] The clusters were generated in the co-expansion of vapor from HNO_3 solution (65%, Sigma-Aldrich) with a buffer gas (He, 99.996%, Messer). The reservoir and nozzle temperatures were $T_R/T_N = 70°C/100°C$ and the helium buffer pressure was 1 bar. These conditions correspond to an HNO_3/H_2O gas phase ratio of ≈0.4 in the reservoir as can be derived from the measurements of the vapor phase above HNO_3/H_2O solutions.[9] After recording the mass spectra for the concentrated nitric acid (65%, 3 mL), the solution was diluted by adding water (3 mL, then 6 mL) through the inlet line into the source reservoir. Thereby, solutions with a nitric acid concentration of ≈ 33% and 16%, respectively, were produced as determined from the ratio of HNO_3 and H_2O in the vapor phase.[9]

The clusters generated in a supersonic expansion passed through the skimmer, and subsequently the beam passed through three differentially pumped vacuum chambers until it reached a perpendicularly mounted reflectron time-of-flight mass spectrometer (TOF). The flight path from the end of the pickup chamber to the ionization region of the TOF was approximately 1.5 m corresponding to the clusters flight time of about 1 ms (the measured cluster velocity was about 1400 ms^{-1}).

In the TOF ionizer, the cluster beam was crossed by an electron beam from a pulsed electron gun. The beam was operated at an 8 kHz frequency with a 2 μs pulse duration, followed by a 0.5 μs delay after each pulse to avoid any ionization by scattered electrons accelerated by the extraction voltage. The negative ions were then extracted by a +5 kV pulse, which was applied for 2 μs. After extraction, the ions were accelerated with +8 kV and passed through an ≈ 95 cm long TOF flight path. The spectra were subsequently recorded with a Photonics MCP detector. The mass spectra were recorded in electron energy scanning mode in the range $0 - 15$ eV with a 0.20 eV step. From these spectra, the electron energy-dependent ion yield curves were obtained for different ions. The electron-energy scale was calibrated using the 4.4 eV and 8.2 eV resonance in the O^- generation from CO_2.[10] Although we use a weak permanent magnetic field to guide the electron beam through the ionization region, our electron gun was not originally designed to work at very low electron energies. Due to the space charge, the electron energy and current cannot be very reliable at electron energies below approximately 1.5 eV, and thus the ion yield (normalized by the electron current) below 1.5 eV is omitted in our spectra as discussed also in our previous work.[8] For a high signal-to-noise ratio, the mass spectra presented in Fig. 1 in the main article were recorded for a longer time at a constant electron energy of 1.5 eV.

1.1. Mass discrimination

The perpendicular TOF arrangement leads inevitably to a mass discrimination. In a supersonic expansion, all the neutral clusters attain essentially the same velocity. In the present case of pure water vapor expansion, the cluster beam velocity was $v \approx 1400$ ms^{-1},[11] and $v \approx 1800$ ms^{-1} for the HNO_3/H_2O co-expansion,[12] with the speed ratio $S \approx 1.6 \times v/\Delta v \approx$ 20-30. This narrow velocity distribution leads to very different kinetic energies for clusters of different sizes, i.e. with different masses. Since the clusters, after their ionization, are extracted perpendicularly to the beam velocity direction, a deflection voltage has to be applied to compensate for the cluster momentum in the direction of the neutral beam velocity. Nevertheless, the spatial spread of the clusters of different sizes (masses) is relatively large and can be only partly compensated by recording the ions on a large area MCP detector (4 cm in diameter). Our previous investigations of water clusters have shown that a portion of the mass spectra of about 0-600 m/z can be recorded without any discrimination.[13] Indeed, this range could be shifted along the m/z axis to larger m/z, but then the smaller masses would be discriminated. Thus, the entire cluster size distribution of the relatively large clusters spanning several thousands of m/z units investigated in the present experiment cannot be recorded without mass discrimination. Nevertheless, this does not influence the present results since the relative changes in the cluster size distribution are apparent in the recorded part of the spectrum.

1.2. Number of picked-up HNO_3 molecules

We can determine the mean number of collisions between a water cluster and a HNO_3 molecule for the $(H_2O)_N$ cluster of the mean size $\bar{N} \approx 180$. To this end, we first calculate the cluster geometrical cross section using equations (1) and (2), where $R_0 = 0.198$ nm can be calculated from the water ice density.[6] From the cluster cross section σ, we can evaluate the number of the cluster collisions n_{col} with the vapor molecules in the pickup chamber on the flight path length $L = 17$ cm using equation (3). We consider the pickup pressure $p = 4 \times 10^{-4}$ mbar and the temperature $T = 300$ K (k_B is the Boltzmann constant). However, it has to be considered that not all the molecules in the vapor in the pickup cell are HNO_3 molecules, since we evaporate HNO_3/H_2O mixture into the cell. Therefore, we divide the number of collisions n_{col} for pure HNO_3 by the vapor pressure ratio $a = 2.47$ between H_2O and HNO_3 in the gas phase for the 65% nitric acid at the evaporation temperature of 50°C,[9] equation (4). Thus the number of collisions of an average size cluster with the HNO_3 corresponds to $n_{col,HNO_3} \approx 0.6$, i.e., the probability of the pickup of an HNO_3 molecule by the average cluster is less than one and thus it can be safely assumed that the majority of the clusters investigated here adsorbed only one HNO_3 molecule.

$$R_N = N^{\frac{1}{3}} R_0 \tag{1}$$

$$\sigma = \pi R_N^2 \tag{2}$$

$$n_{col} = \sigma L \frac{p}{k_B T} \tag{3}$$

$$n_{col,HNO_3} = \frac{n_{col}}{a} \tag{4}$$

It should be mentioned that in our previous investigations we have realized that the pickup cross section can exceed the geometrical cross section for water clusters.[11] In addition, there are larger clusters in the entire cluster size distribution, which could undergo more than one collision with the HNO_3 molecules in the pickup cell. Nevertheless, it is possible that not all collisions with the HNO_3 are sticky and, more importantly, we analyze rather smaller clusters from the entire cluster size distribution in the mass spectra (see the mass discrimination above). Therefore, it can be safely assumed that the majority of the clusters investigated here, picked up just a single HNO_3 molecule.

2. Isobaric ions

When discussing the mass spectra, mass coincidences (isobaric ions) should be considered, since $m/z = 126$ is the same for 2×HNO_3 and 7×H_2O. This mass coincidence is of particular importance when it comes to the series with an odd number of HNO_3 molecules and one NO_3^- ion, as it would coincide with the OH^- series in our spectra, i.e., $(HNO_3)_{2k+1}(H_2O)_n NO_3^-$ peaks coincide with $(H_2O)_{n+7k+6}OH^-$ peaks. These isobars pose a challenge for our data evaluation, and their assignment to single species is important, as the NO_3^- and OH^- series represent the fingerprints of acid dissociation and non-dissociated HNO_3 molecules, respectively. There are further mass coincidences within the NO_3^- and OH^- series separately, which play a less important role in our case, where the clusters can contain either $2k\times$ HNO_3 or $7k\times$ H_2O molecules, i.e., $(HNO_3)_{2k}(H_2O)_n NO_3^-$ coincides with $(H_2O)_{n+7k}NO_3^-$, and $(HNO_3)_{2k}(H_2O)_n OH^-$ has the same mass as $(H_2O)_{n+7k}OH^-$.

In order to exclude the contribution of isobars in our spectra, we conducted a thorough investigation of the ion peaks that were suspected to be the result of mass coincidences. Our approach and findings can be summarized as follows:

(i) We determined the mean number of collisions between a water cluster and an HNO_3 molecule by calculations above (Section 1.2). As outlined above, the pickup of more than one HNO_3 is highly unlikely and the contribution from isobars resulting from clusters containing multiple HNO_3 molecules, i.e., $(HNO_3)_m(H_2O)_nNO_3^-$ with $m \geq 1$, is negligible.

(ii) We recorded a high resolution spectrum in which we were able to distinguish the exact masses, i.e., $(HNO_3)_2H^+$ at $m/z = 126.999$ from $(H_2O)_7H^+$ at $m/z = 127.082$, previously.[6] Thus we performed the high resolution scan for the present spectra as well. Indeed, the corresponding intensities are significantly lower when the TOF is tuned to the high resolution mode. The spectrum of peaks suspected to contain isobaric ions is displayed in Figure 1. If the peaks were composed of two contributions with comparable intensities separated by about 0.1 m/z, it should be reflected in the present peak shape, which is not the case.

(iii) We investigated the peak intensity dependence on the HNO_3 pickup pressure (see Fig. 2). The peaks corresponding to the HNO_3 pickup should exhibit a different dependence on the pickup pressure than the peaks issuing simply from the water clusters. There is no significant difference in dependence between peaks that could possibly contain an isobar contribution, such as at m/z = 143 ($(H_2O)_7OH^-$ or $HNO_3(H_2O)NO_3^-$) and those unambiguously assigned to one product, e.g., $(H_2O)_6OH^-$.

Therefore we argue that the discussed ion peaks that we observe in our mass spectra can be exclusively assigned to the $(H_2O)_nOH^-$ and $(H_2O)_nNO_3^-$ series separately.

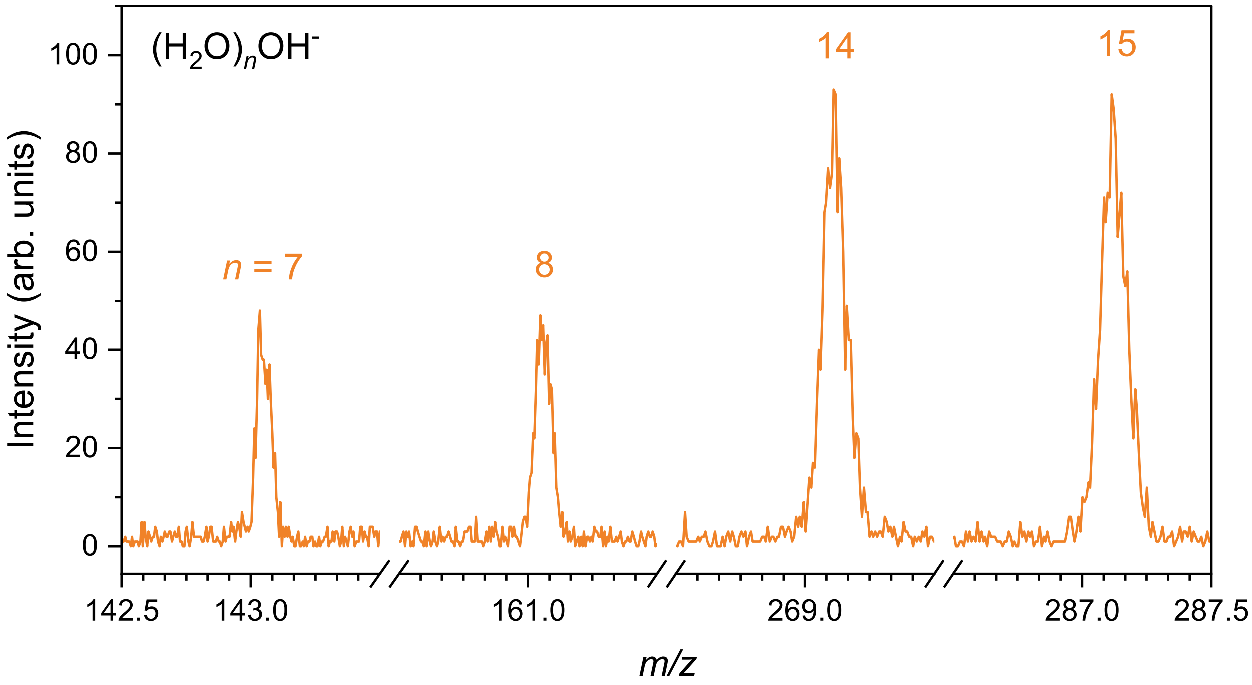

Figure 1. High resolution mass spectrum of the mass peaks suspected to contain isobaric ions.

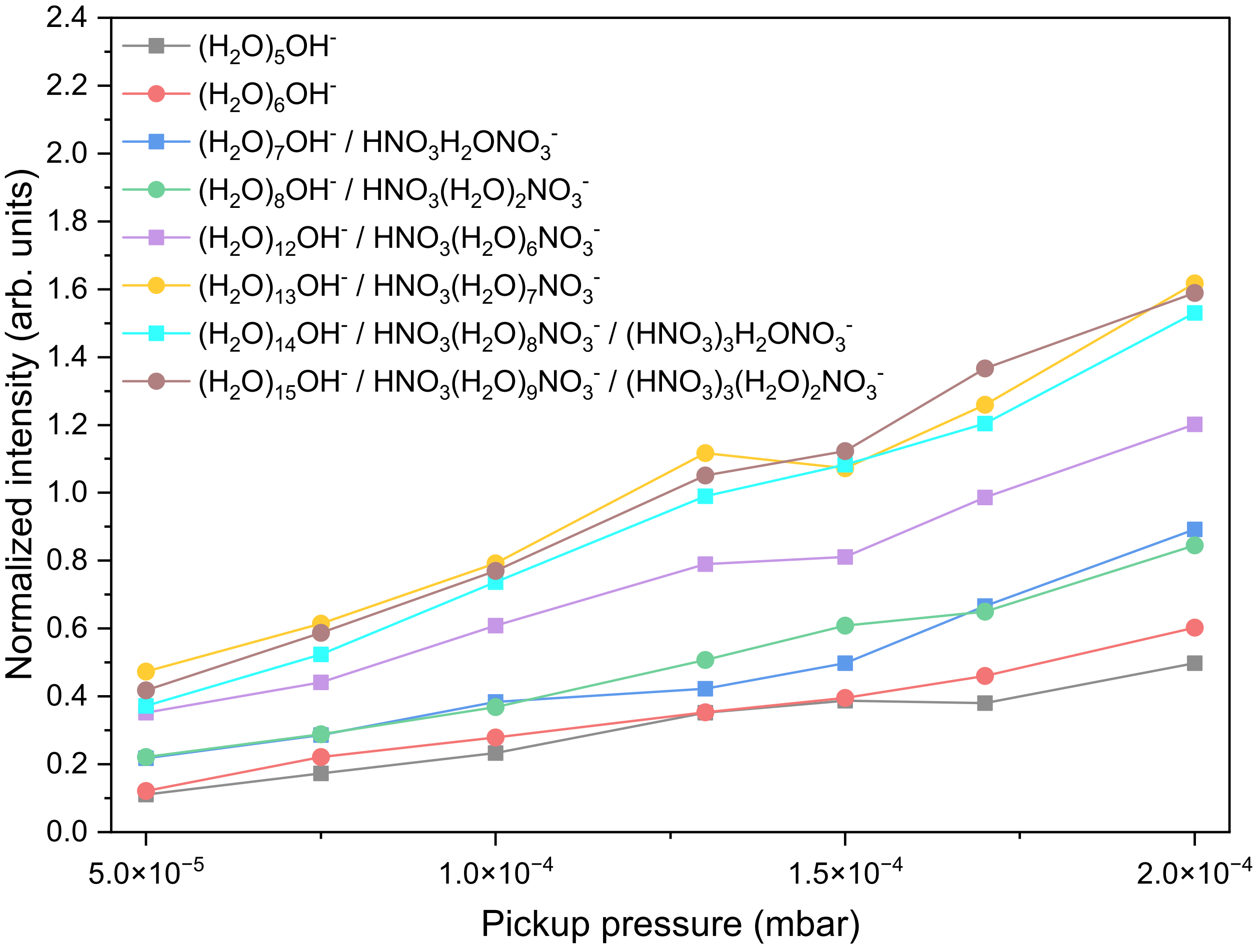

Figure 2. Pickup pressure dependence of several peaks suspected to contain an isobar contribution. The spectra have been normalized to the $(H_2O)_{21}{}^-$ peak intensity.

3. Metastable clusters

In the mass spectrum in Fig. 1 in the main paper, the pure water clusters exhibit metastable mass peaks labeled by stars. They correspond to the evaporation of a water molecule from the already ionized cluster in the first field free region of the TOF. Immediately after the ionization, the clusters may fragment on a time scale significantly shorter than the time spent by the ion in the extraction region of the TOF ($\leq$1 ns). These cluster ion fragments appear at the mass spectrum at the exact m/z corresponding to the cluster ions (strictly speaking, the cluster ions that fragment fast still on their way out of the extraction region appear as 'peak tails' towards higher masses). However, individual water molecules can evaporate from the cluster ions during their flight time in the first field-free region of the TOF, which takes place on the time scale of tens of microseconds. Thus, they enter the reflectron as different masses from the original ones, which were accelerated in the ion source. These mass peaks appear typically at fractional masses. The position of these peaks with respect to the stable ions depends on the voltages in the reflectron, which can be exploited in their identification, which we have done for the pure water clusters.

This method to investigate metastable fragmentation using a reflectron time-of-flight mass spectrometer was described previously in Ref. 14 and in references cited therein. The evaporation of one to several water molecules from the cluster ions on the μs-time scale, termed metastable fragmentation, was observed for positively charged water clusters $(H_2O)_nH^+$ previously.[15] Recently, we have done similar experiments with both positively and negatively charged large water clusters, which confirmed the peaks labeled by stars in Fig. 1 in the main article as the metastable peaks, i.e., corresponding to the $(H_2O)_n^-$ ions from which one water molecule was evaporated during its flight time through the first field free region of the TOF, which takes up to about 20 μs.

4. Cluster size and temperature

In the main manuscript, we showed and discussed mainly the HNO_3 pickup spectrum corresponding to a reservoir/nozzle temperature of $T_R/T_N = 130°\mathrm{C}$ / $160°\mathrm{C}$, i.e., $\bar{N} \approx 180$. We also conducted additional HNO_3 pickup experiments at varying expansion conditions (see Table 1). The main aim was to examine the dependence of the occurring processes on the cluster size and eventually on their temperature. The mass spectra at each condition are displayed in Figure 3. Qualitatively, all the spectra are essentially the same, exhibiting the same ion series. The cluster temperatures from the literature were based on semiempirical model[16] and as such can be only regarded as approximate. Therefore, we do not derive any conclusions about the degree of the acid dissociation from the spectra correlated with the cluster temperature.

Table 1. Various investigated experimental conditions. The $(H_2O)_nNO_3^-$ to $(H_2O)_nOH^-$ peak intensity ratio (last column) is an average for $n = 10 - 30$.

Condition	Compounds	T_R (°C)	T_N (°C)	p_{H_2O} (bar)	N	r_N[6] (Å)	T_C[16] (K)	NO_3^-: OH^-
A	$H_2O + HNO_3$	100	160	0.99	30	6.63	177[a]	0.300
B	$H_2O + HNO_3$	130	160	2.63	180	12.05	106[b]	0.398
C	$H_2O + HNO_3$	130	140	2.63	220	12.88	-	0.400
D	$H_2O + HNO_3$	150	160	4.62	470	16.59	93[c]	0.474

[a] literature value for $p_{H_2O} = 1.2$ bar and $N = 47$. [b] literature value for $p_{H_2O} = 2.6$ bar and $N = 181$. [c] literature value for $p_{H_2O} = 4.8$ bar and $N = 526$.

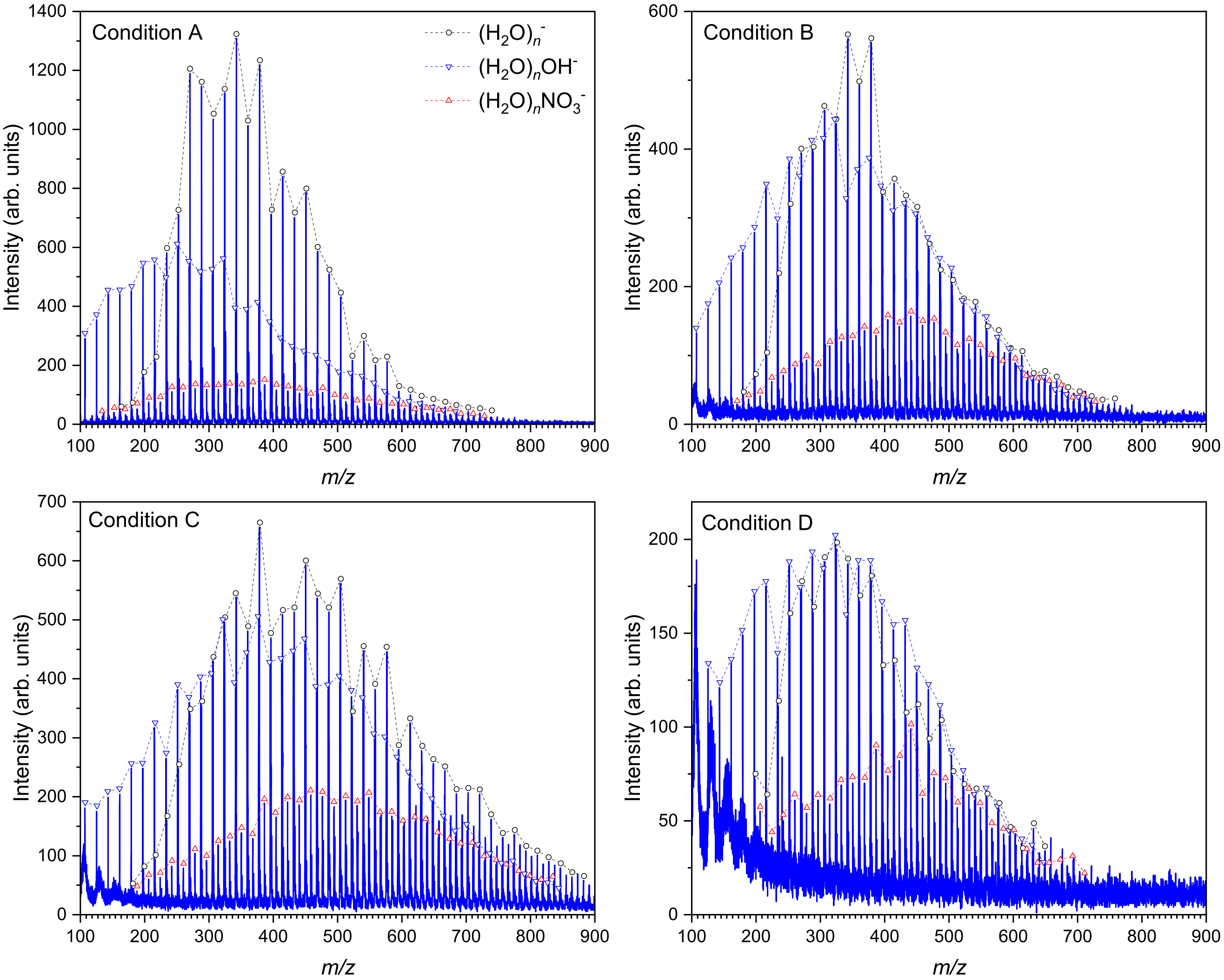

Figure 3. Mass spectra of HNO_3 pickup experiments conducted at several conditions. The mean cluster size increases from Condition A to D. The black circles represent $(H_2O)_n{}^-$, the blue upward triangle $(H_2O)_nOH^-$ and the red downward triangle the $(H_2O)_nNO_3{}^-$ peak series.

References

[1] M. Fárník, J. Lengyel, *Mass Spectrom. Rev.* **2018**, *37*, 630.

[2] M. Fárník, J. Fedor, J. Kočišek, J. Lengyel, E. Pluhařová, V. Poterya, A. Pysanenko, *Phys. Chem. Chem. Phys.* **2021**, *23*, 3195.

[3] M. Fárník, *J. Phys. Chem. Lett.* **2023**, *14*, 287.

[4] C. Bobbert, S. Schütte, C. Steinbach, U. Buck, *Eur. Phys. J. D* **2002**, *19*, 183.

[5] O. F. Hagena, *Surf. Sci.* **1981**, *106*, 101.

[6] J. Lengyel, A. Pysanenko, J. Kočišek, V. Poterya, C. C. Pradzynski, T. Zeuch, P. Slavíček, M. Fárník, *J. Phys. Chem. Lett.* **2012**, *3*, 3096.

[7] J. Lengyel, M. Ončák, J. Fedor, J. Kočišek, A. Pysanenko, M. K. Beyer, M. Fárník, *Phys. Chem. Chem. Phys.* **2017**, *19*, 11753.

[8] J. Lengyel, J. Fedor, M. Fárník, *Phys. Chem. Chem. Phys.* **2019**, *21*, 8691.

[9] G. B. Taylor, *Ind. Eng. Chem.* **1925**, *17*, 633.

[10] S. Denifl, V. Vizcaino, T. D. Märk, E. Illenberger, P. Scheier, *Phys. Chem. Chem. Phys.* **2010**, *12*, 5219.

[11] J. Lengyel, J. Kočišek, V. Poterya, A. Pysanenko, P. Svrčková, M. Fárník, D. K. Zaouris, J. Fedor, *J. Chem. Phys.* **2012**, *137*, 034304.

[12] A. Pysanenko, J. Lengyel, M. Fárník, *J. Chem. Phys.* **2018**, *148*, 154301.

[13] J. Lengyel, A. Pysanenko, V. Poterya, J. Kočišek, M. Fárník, *Chem. Phys. Lett.* **2014**, *612*, 256 .

[14] S. Q. Wei, A. W. Castleman, *Int. J. Mass Spectrom. Ion Processes* **1994**, *131*, 233.

[15] L. Belau, K. R. Wilson, S. R. Leone, M. Ahmed, *J. Phys. Chem. A* **2007**, *111*, 10075.

[16] D. Becker, C. W. Dierking, J. Suchan, F. Zurheide, J. Lengyel, M. Fárník, P. Slavíček, U. Buck, T. Zeuch, *Phys. Chem. Chem. Phys.* **2021**, *23*, 7682.